Discrete effect on the halfway bounce-back boundary condition of multiple-relaxation-time lattice Boltzmann model for convection-diffusion equations

Shuqi Cui,[1] Ning Hong,[2] Baochang Shi,[1,3] and Zhenhua Chai[1,3,*]

[1]*School of Mathematics and Statistics, Huazhong University of Science and Technology, Wuhan 430074, China*

[2]*School of Information and Engineering, Wuchang University of Technology, Wuhan 430223, China*

[3]*State Key Laboratory of Coal Combustion, Huazhong University of Science and Technology, Wuhan 430074, China*

(Received 11 November 2015; revised manuscript received 25 March 2016; published 13 April 2016)

In this paper, we will focus on the multiple-relaxation-time (MRT) lattice Boltzmann model for two-dimensional convection-diffusion equations (CDEs), and analyze the discrete effect on the halfway bounce-back (HBB) boundary condition (or sometimes called bounce-back boundary condition) of the MRT model where three different discrete velocity models are considered. We first present a theoretical analysis on the discrete effect of the HBB boundary condition for the simple problems with a parabolic distribution in the x or y direction, and a *numerical* slip proportional to the second-order of lattice spacing is observed at the boundary, which means that the MRT model has a second-order convergence rate in space. The theoretical analysis also shows that the *numerical* slip can be eliminated in the MRT model through tuning the free relaxation parameter corresponding to the second-order moment, while it cannot be removed in the single-relaxation-time model or the Bhatnagar-Gross-Krook model unless the relaxation parameter related to the diffusion coefficient is set to be a special value. We then perform some simulations to confirm our theoretical results, and find that the numerical results are consistent with our theoretical analysis. Finally, we would also like to point out the present analysis can be extended to other boundary conditions of lattice Boltzmann models for CDEs.

DOI: 10.1103/PhysRevE.93.043311

I. INTRODUCTION

Over the past decades, the lattice Boltzmann (LB) method, as a numerical approach developed from the simplified kinetic models, has gained great success in the simulation of the complex flows, and has also been used to solve the diffusion and convection-diffusion equations (CDEs) for their importance in the study of heat and mass transfer [1–3]. Although there are many works on the LB method for CDEs [4–29], the discrete effect on the boundary condition, as a fundamental problem in the LB method for CDEs, has not been investigated comprehensively. To our knowledge, there are some available works on the discrete effects of the boundary conditions [30–36]. Ginzburg and Adler first performed a boundary condition analysis for the face-centered-hypercube LB model, and demonstrated that for the Poiseuille flow, the commonly used halfway bounce-back (HBB) boundary condition brings an error with a second-order accuracy in space, which can be eliminated through tuning the free eigenvalue of the collision matrix [30]. He *et al.* also conducted an analysis on the discrete effects of boundary conditions for the Bhatnagar-Gross-Krook (BGK) model, and found that the HBB boundary condition indeed yields a nonzero slip on a solid wall, which is of second-order accuracy in space [31]. Following a similar way, Guo *et al.* [32,33] further analyzed the discrete effects on Maxwell's diffuse reflection [37] and combined HBB and specular-reflection boundary conditions [38] for microscale gas flows, and also observed that there is a *numerical* slip depending on the grid number. To implement an exact slip boundary condition in the LB model, they also proposed a strategy to correct the discrete effect. However, it should be noted that Maxwell's diffuse reflection and combined HBB and specular-reflection boundary conditions considered in Refs. [32,33] are nonlocal, and hence they are not suitable for fluid flow in a complex geometry. To overcome the limitation of the above nonlocal boundary conditions, Chai *et al.* developed a local combined HBB and full diffusive boundary condition for microscale gas flows in complex geometries [34,35], and also carried out an analysis on the discrete effect of the combined boundary condition. The results in this work illustrated that to realize the exact slip boundary condition, the discrete effect must also be included and corrected. Recently, Prasianakis *et al.* [36] also conducted an analysis of the three-dimensional BGK model with the HBB boundary condition for the Poiseuille flow, and their results are similar to those of the two-dimensional BGK model with nine discrete velocities [31]. However, we noted that all of above works are limited to the HBB boundary conditions of the LB method for fluid flows.

Recently, Zhang *et al.* presented a general HBB boundary condition of the BGK model for CDEs, and also performed an analysis on the discrete effect of the HBB boundary condition [39]. The results in their work show that for the diffusion in Poiseuille flow, the *numerical* slip is zero since distribution of the concentration is only a linear function of the y coordinate, while for the diffusion in Couette flow with wall injection, a nonzero *numerical* slip related to lattice spacing or grid number is observed, and cannot be removed in the BGK model. In this work, we will consider the discrete effect on the HBB boundary condition of the multiple-relaxation-time (MRT) model for CDEs, and both theoretical analysis and numerical results show that for the simple problems with a parabolic distribution in one (x or y) direction, the discrete effect on the HBB boundary condition can be eliminated through tuning the free relaxation parameter. Besides, we also present a comparison between the BGK model and MRT model, and the results also show that the MRT model could be more accurate than the BGK model.

*Corresponding author: hustczh@hust.edu.cn

The rest of paper is organized as follows. In Sec. II, the MRT model for the CDE with a source term is first introduced; then a theoretical analysis on the discrete effect of the BB boundary condition is performed in Sec. III. In Sec. IV, the numerical results and discussion are presented, and finally, some conclusions are given in Sec. V.

II. MULTIPLE-RELAXATION-TIME LATTICE BOLTZMANN MODEL FOR TWO-DIMENSIONAL CONVECTION-DIFFUSION EQUATIONS

A. Two-dimensional convection-diffusion equation

The convection-diffusion equation is a combination of convection and diffusion equations, and is usually used to describe the physical phenomena during the convection and diffusion process. It has also received a great deal of research attention for its important role in the study of mass and heat transfer [40]. The two-dimensional convection-diffusion equation with a source term can be written as

$$\partial_t \phi + \nabla \cdot (\phi \mathbf{u}) = \nabla \cdot (D \nabla \phi) + R, \tag{1}$$

where ϕ is a scalar variable and is a function of time and space, ∇ is the gradient operator, and D is the diffusion coefficient. $\mathbf{u} = (u_x, u_y)^\top$ is the convection velocity with $\top$ denoting the transpose of a vector or matrix, and $R(\mathbf{x},t)$ is the source term.

B. Multiple-relaxation-time lattice Boltzmann model

In the framework of the LB method, the models can be classified into several kinds, i.e., the BGK model [41], entropic LB model [42–44], quasiequilibrium LB model [45,46], two-relaxation-time model [19,29], central moment or cascaded LB model [47,48], and MRT model [49,50]. In this work, we will consider the MRT model since it is a generalized LB model, and has more free relaxation parameters that can be used to improve the stability and accuracy of the LB method.

The evolution equation of the MRT model for the CDE [Eq. (1)] can be written as [15]

$$\begin{aligned} & f_i(\mathbf{x} + \mathbf{c}_i \delta t,\, t + \delta t) \\ &= f_i(\mathbf{x},\, t) - (\mathbf{M}^{-1}\mathbf{S}\mathbf{M})_{ik}\left[f_k(\mathbf{x},\, t) - f_k^{(\mathrm{eq})}(\mathbf{x},\, t)\right] \\ &\quad + \delta t \left[\mathbf{M}^{-1}\left(\mathbf{I} - \frac{\mathbf{S}}{2}\right)\mathbf{M}\right]_{ik} R_k, \quad i = 0, \ldots, q-1, \end{aligned} \tag{2}$$

where δt is time step, $\mathbf{I}$ is the unit matrix, and $\mathbf{S}$ is a diagonal relaxation matrix with non-negative elements. $f_i(\mathbf{x},\, t)$ is the distribution function associated with the discrete velocity $\mathbf{c}_i$ at position $\mathbf{x}$ and time t, $f_i^{(\mathrm{eq})}(\mathbf{x},\, t)$ is equilibrium distribution function (EDF), and for simplicity, only the linear EDF is considered here,

$$f_i^{(\mathrm{eq})}(\mathbf{x},\, t) = \omega_i \phi \left(1 + \frac{\mathbf{c}_i \cdot \mathbf{u}}{c_s^2}\right), \tag{3}$$

where ω_i is the weight coefficient, and c_s is the so-called lattice speed. R_i is the discrete source term, and can be defined as

$$R_i = \omega_i R. \tag{4}$$

$\mathbf{M}$ is the transformation matrix, and is used to project the distribution function f_i and EDF $f_i^{(\mathrm{eq})}$ in the velocity space onto the macroscopic variables in the moment space [49,51,52],

$$\mathbf{m} := \mathbf{M}\mathbf{f}, \quad \mathbf{m}^{(\mathrm{eq})} := \mathbf{M}\mathbf{f}^{(\mathrm{eq})}, \tag{5}$$

where $\mathbf{f} = (f_0, \ldots, \phi_{q-1})^\top$, $\mathbf{f}^{(\mathrm{eq})} = (f_0^{(\mathrm{eq})}, \ldots, f_{q-1}^{(\mathrm{eq})})^\top$ with q representing the number of discrete velocity directions.

In different discrete lattice (DdQq: D denotes the dimensional space with the value $d = 2$, Q represents the discrete velocity direction with the number q) models, the discrete velocity $\mathbf{c}_i$, the weight coefficient ω_i, the speed c_s, the transportation matrix $\mathbf{M}$, and the diagonal relaxation matrix $\mathbf{S}$ can be given by the following equations.

D2Q4 lattice model:

$$\mathbf{c} = \begin{pmatrix} 1 & 0 & -1 & 0 \\ 0 & 1 & 0 & -1 \end{pmatrix} c, \tag{6a}$$

$$\omega_i = 1/4 \ \ (i = 1 \text{ to } 4), \quad c_s^2 = \frac{1}{2}c^2, \tag{6b}$$

$$\mathbf{M} = \mathbf{C}_d \mathbf{M}_0, \quad \mathbf{S} = \mathrm{diag}(s_0, s_1, s_1, s_2), \tag{6c}$$

$$\mathbf{C}_d = \mathrm{diag}(1, c, c, c^2), \quad \mathbf{M}_0 = \begin{pmatrix} 1 & 1 & 1 & 1 \\ 1 & 0 & -1 & 0 \\ 0 & 1 & 0 & -1 \\ 1 & -1 & 1 & -1 \end{pmatrix}. \tag{6d}$$

D2Q5 lattice model:

$$\mathbf{c} = \begin{pmatrix} 0 & 1 & 0 & -1 & 0 \\ 0 & 0 & 1 & 0 & -1 \end{pmatrix} c, \tag{7a}$$

$$\omega_i = 1/5 \ \ (i = 0 \text{ to } 4), \quad c_s^2 = \frac{2}{5}c^2, \tag{7b}$$

$$\mathbf{M} = \mathbf{C}_d \mathbf{M}_0, \quad \mathbf{S} = \mathrm{diag}(s_0, s_1, s_1, s_2, s_2), \tag{7c}$$

$$\mathbf{C}_d = \mathrm{diag}(1, c, c, c^2, c^2),$$

$$\mathbf{M}_0 = \begin{pmatrix} 1 & 1 & 1 & 1 & 1 \\ 0 & 1 & 0 & -1 & 0 \\ 0 & 0 & 1 & 0 & -1 \\ 0 & 1 & -1 & 1 & -1 \\ -4 & 1 & 1 & 1 & 1 \end{pmatrix}. \tag{7d}$$

D2Q9 lattice model:

$$\mathbf{c} = \begin{pmatrix} 0 & 1 & 0 & -1 & 0 & 1 & -1 & -1 & 1 \\ 0 & 0 & 1 & 0 & -1 & 1 & 1 & -1 & -1 \end{pmatrix} c, \tag{8a}$$

$$\omega_0 = 4/9, \ \omega_{k=1 \text{ to } 4} = 1/9, \ \omega_{k=5 \text{ to } 8} = 1/36, \quad c_s^2 = \tfrac{1}{3}c^2, \tag{8b}$$

$$\mathbf{M} = \mathbf{C}_d \mathbf{M}_0, \quad \mathbf{S} = \mathrm{diag}(s_0, s_5, s_4, s_1, s_3, s_1, s_3, s_2, s_2), \tag{8c}$$

$$\mathbf{C}_d = \mathrm{diag}(1, c^2, c^4, c, c^3, c, c^3, c^2, c^2),$$

$$\mathbf{M}_0 = \begin{pmatrix} 1 & 1 & 1 & 1 & 1 & 1 & 1 & 1 & 1 \\ -4 & -1 & -1 & -1 & -1 & 2 & 2 & 2 & 2 \\ 4 & -2 & -2 & -2 & -2 & 1 & 1 & 1 & 1 \\ 0 & 1 & 0 & -1 & 0 & 1 & -1 & -1 & 1 \\ 0 & -2 & 0 & 2 & 0 & 1 & -1 & -1 & 1 \\ 0 & 0 & 1 & 0 & -1 & 1 & 1 & -1 & -1 \\ 0 & 0 & -2 & 0 & 2 & 1 & 1 & -1 & -1 \\ 0 & 1 & -1 & 1 & -1 & 0 & 0 & 0 & 0 \\ 0 & 0 & 0 & 0 & 0 & 1 & -1 & 1 & -1 \end{pmatrix}, \tag{8d}$$

where $c = \delta x/\delta t$ with δx representing the lattice spacing. Besides, based on Eqs. (6c), (7c), and (8c), one can easily obtain the relation $\mathbf{M}^{-1}\mathbf{S}\mathbf{M} = \mathbf{M}_0^{-1}\mathbf{S}\mathbf{M}_0$; then the evolution equation can be rewritten as

$$\begin{aligned} &f_i(\mathbf{x}+\mathbf{c}_i\delta t,\, t+\delta t) \\ &\quad = f_i(\mathbf{x},\, t) - \left(\mathbf{M}_0^{-1}\mathbf{S}\mathbf{M}_0\right)_{ik}\left[f_k(\mathbf{x},\, t) - f_k^{(\mathrm{eq})}(\mathbf{x},\, t)\right] \\ &\qquad + \delta t\left[\mathbf{M}_0^{-1}\left(\mathbf{I}-\frac{\mathbf{S}}{2}\right)\mathbf{M}_0\right]_{ik} R_k. \end{aligned} \tag{9}$$

It should be noted that in the MRT model, the evolution process can also be decomposed into two steps, i.e., collision and propagation, and usually the collision step is implemented in the moment space [50], while to simplify the following analysis on the discrete effect of the HBB boundary condition, here the collision and propagation steps are expressed by the following equations,

$$\begin{aligned} f_i^{+}(\mathbf{x},\, t) = f_i(\mathbf{x},\, t) &- \left(\mathbf{M}_0^{-1}\mathbf{S}\mathbf{M}_0\right)_{ik} \\ &\times \left[f_k(\mathbf{x},\, t) - f_k^{(\mathrm{eq})}(\mathbf{x},\, t)\right] \\ &+ \delta t\left[\mathbf{M}_0^{-1}\left(\mathbf{I}-\frac{\mathbf{S}}{2}\right)\mathbf{M}_0\right]_{ik} R_k, \end{aligned} \tag{10a}$$

$$f_i(\mathbf{x}+\mathbf{c}_i\delta t,\, t+\delta t) = f_i^{+}(\mathbf{x},\, t), \tag{10b}$$

where $f_i^{+}(\mathbf{x},\, t)$ is postcollision distribution function.

The macroscopic variable ϕ in the present MRT model should be computed by

$$\phi(\mathbf{x},\, t) = \sum_i f_i(\mathbf{x},\, t) + \frac{\delta t}{2}R. \tag{11}$$

where the source term effect has been included. Through the Chapman-Enskog analysis [15] or the asymptotic analysis [21], the CDE with a source term, i.e., Eq. (1), can be recovered from the MRT model with the following diffusion coefficient,

$$D = \left(\frac{1}{s_D} - \frac{1}{2}\right)c_s^2\delta t, \tag{12}$$

where $s_D = s_1$ is the relaxation parameter related to the diffusion coefficient. Finally, we would also like to point out that in the Chapman-Enskog analysis, the relaxation parameter s_0 has no influence on the derivation of the CDE, and also, if the relaxation parameters $s_i (i = 0 \text{ to } 8)$ are equal to each other and are given by s_D, the MRT model will reduce to the BGK model.

III. DISCRETE EFFECT ON THE HALFWAY BOUNCE-BACK BOUNDARY CONDITION OF MRT MODEL FOR CDE

As stated previously, the discrete effects on the boundary conditions of the BGK or MRT model for the Navier-Stokes equations have been studied extensively [30–35], while the discrete effect on the boundary condition of the MRT model for CDEs is still unclear. To fill the gap, we will present a detailed analysis on the discrete effect of the HBB boundary condition in the framework of the MRT model for CDEs.

A. Equivalent finite-difference scheme of the MRT model for some simple problems

In this section, we only consider the steady or time-independent problems satisfying

$$\frac{\partial\phi}{\partial t} = 0,\ \ \frac{\partial\phi}{\partial x} = 0,\ \ \frac{\partial u_x}{\partial x} = \frac{\partial u_y}{\partial x} = 0,\ \ R = \text{const.} \tag{13}$$

Based on Eq. (13), one can find that the scalar variable ϕ, velocity $\mathbf{u}$, and the distribution function should be only functions of the y coordinate. We note that although the problems considered above are very simple, they can be served as an example for us to present theoretical analysis and derive the equivalent finite-difference scheme of the MRT model.

Without a loss of generality, here we consider the MRT model with the D2Q4 lattice,

$$\begin{aligned} &f_i(\mathbf{x}+\mathbf{c}_i\delta t,\, t+\delta t) \\ &\quad = f_i(\mathbf{x},\, t) - \left(\mathbf{M}_0^{-1}\mathbf{S}\mathbf{M}_0\right)_{ik}\left[f_k(\mathbf{x},\, t) - f_k^{(\mathrm{eq})}(\mathbf{x},\, t)\right] \\ &\qquad + \delta t\left[\mathbf{M}_0^{-1}\left(\mathbf{I}-\frac{\mathbf{S}}{2}\right)\mathbf{M}_0\right]_{ik} R_k, \quad i = 1 \text{ to } 4. \end{aligned} \tag{14}$$

Based on this equation and after some algebraic manipulation, one can obtain the following equivalent finite-difference scheme of the MRT model (see Appendix A for details),

$$\frac{\phi_{k+1}u_{y,k+1} - \phi_{k-1}u_{y,k-1}}{2\delta x} = D\frac{\phi_{k-1} - 2\phi_k + \phi_{k+1}}{\delta x^2} + R, \tag{15}$$

where the diffusion coefficient D is given by Eq. (12) with $c_s^2 = c^2/2$.

We now present some remarks on the results shown above.

Remark I. Equation (15) is the equivalent second-order finite-difference scheme of the MRT model for the simplified CDE [Eq. (1)] under the assumptions presented in Eq. (13),

$$\frac{\partial(\phi u_y)}{\partial y} = D\frac{\partial^2\phi}{\partial y^2} + R. \tag{16}$$

Remark II. When the D2Q5 and D2Q9 lattice models are used, the same results as Eq. (15) can also be obtained.

Remark III. From the analysis shown in Appendix A, it is clear that the relaxation parameter s_0 corresponding to the conservative variable ϕ has no influence on the derivation of Eq. (15), and can be chosen arbitrarily when it is less than 2.0. We note that this result is also consistent with that given by the

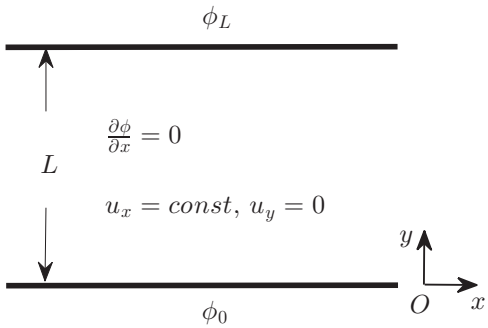

FIG. 1. Schematic of the unidirectional and time-independent diffusion problem.

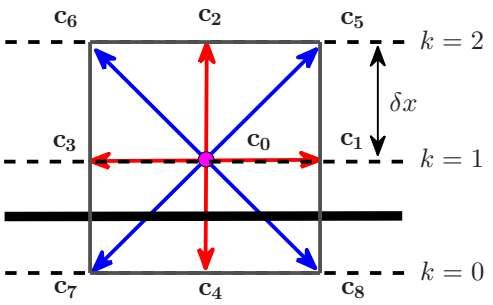

FIG. 2. The boundary arrangement in the D2Qq ($q = 4$, 5, or 9) lattice model; the bold line denotes the bottom boundary and is located at $k = 1/2$.

Chapman-Enskog analysis, and thus, in the following analysis and numerical simulations, $s_0 = 0$ would be used.

B. Discrete effect of the halfway bounce-back boundary condition

To simplify the analysis on the discrete effect of the HBB boundary condition, a unidirectional and time-independent diffusion problem (see Fig. 1 where $\partial_x \phi = 0$, $u_x = \text{const}$, and $u_y = 0$) is adopted, and it can be described by the following simplified equation and boundary conditions,

$$D\frac{\partial^2 \phi}{\partial y^2} + R = 0, \tag{17a}$$

$$\phi(x, y = 0) = \phi_0, \quad \phi(x, y = L) = \phi_L, \tag{17b}$$

where ϕ_0 and ϕ_L are two constants, and L is the width between the top and bottom boundaries. R is the source term and is defined by

$$R = 2D\Delta\phi/L^2, \ \ \Delta\phi = \phi_L - \phi_0. \tag{18}$$

For this simple problem, we can obtain its exact solution,

$$\phi(y) = \phi_0 + \Delta\phi y(2 - y), \tag{19}$$

while when the LB model is used to study this problem, one can also derive its analytical solution,

$$\phi_k = \phi_0 + \Delta\phi y_k(2 - y_k) + \phi_s, \tag{20}$$

where $y_k = (k - 0.5)L/N$ with N representing grid number. ϕ_s is the *numerical* slip caused by the implementation of

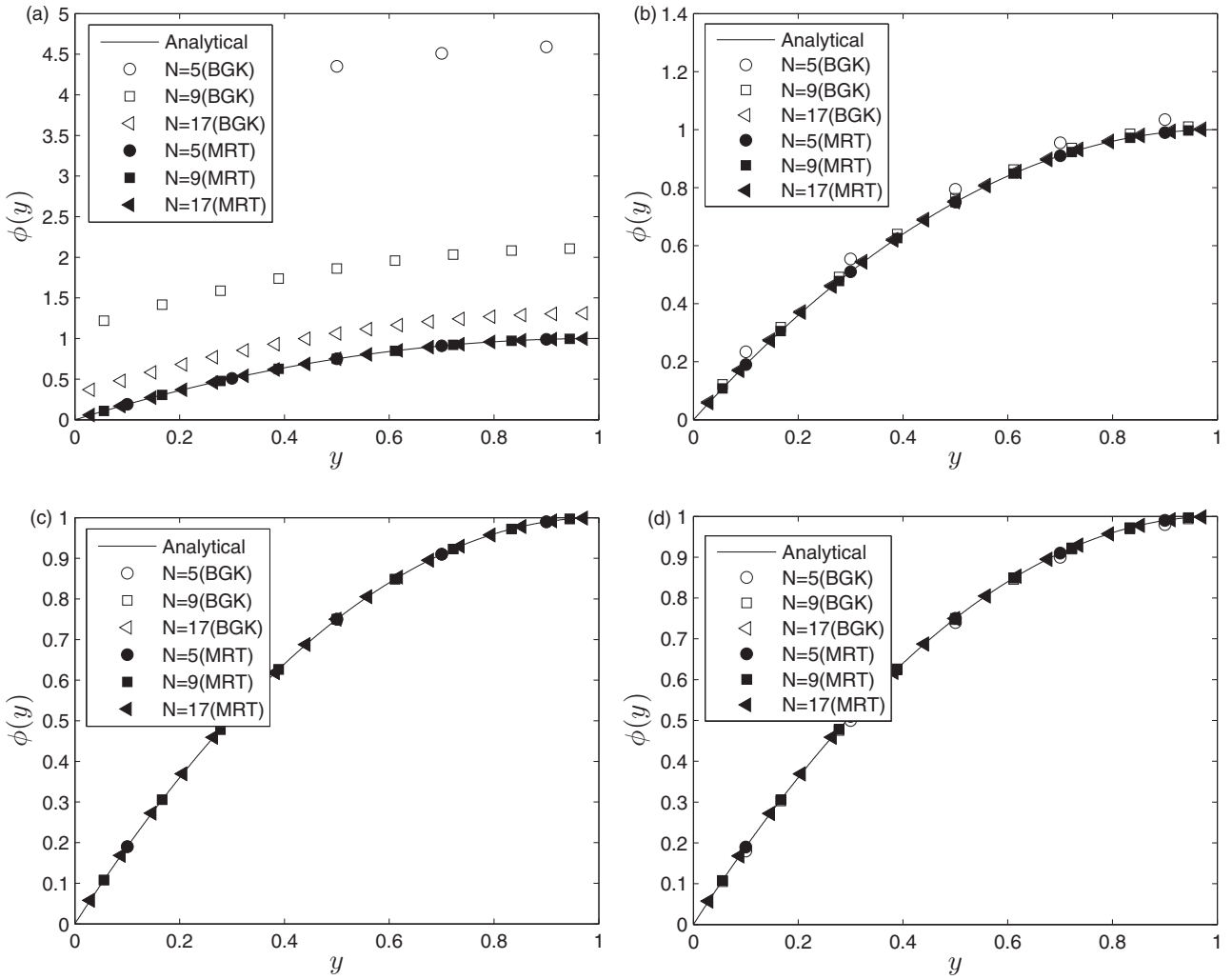

FIG. 3. Numerical results of the BGK and MRT models (D2Q4 lattice) under different lattice sizes and relaxation parameters (a) $s_D = 0.1$, (b) $s_D = 0.6$, (c) $s_D = 1.0$, and (d) $s_D = 1.9$.

the boundary condition or the so-called discrete effect of the boundary condition, and it is the only term that causes the solution of the LB model [Eq. (20)] to be different from the exact solution of the problem [Eq. (19)]. To obtain the *numerical* slip, some proper boundary conditions of the LB method are also needed to treat the Dirichlet boundary conditions (17b). Here we only consider the HBB boundary condition (see Fig. 2) for its locality and second-order convergence rate in space [39,53–56]. When the HBB boundary condition is adopted, the unknown distribution functions at the layer $k = 1$ can be determined by the following equations [39].

D2Q4 or D2Q5 lattice model:

$$f_2^1 = -f_4^{1,+} + 2\omega_4\phi_0. \tag{21}$$

D2Q9 lattice model:

$$f_2^1 = -f_4^{1,+} + 2\omega_4\phi_0, \tag{22a}$$

$$f_5^1 = -f_7^{1,+} + 2\omega_7\phi_0, \tag{22b}$$

$$f_6^1 = -f_8^{1,+} + 2\omega_8\phi_0. \tag{22c}$$

Similar to above analysis, here we also take D2Q4 lattice model as an example, and perform an analysis on the discrete effect of the HBB boundary condition to derive the *numerical* slip ϕ_s (see the details in Appendix B),

$$\phi_{s,\mathrm{MRT}} = \frac{2 - s_1 - s_2}{2s_1s_2}\frac{\Delta\phi}{N^2}. \tag{23}$$

From above equation, it is clear that the HBB boundary condition gives a nonzero *numerical* slip, and has a second-order convergence rate in space since the *numerical* slip $\phi_{s,\mathrm{MRT}}$ has a term of $O(1/N^2)$. Actually, in the MRT model, $\phi_{s,\mathrm{MRT}} = 0$ can be guaranteed if the free relaxation parameter s_2 satisfies the following relation,

$$s_2 = 2 - s_1 = 2 - s_D, \tag{24}$$

which means that the discrete effect of the boundary condition can be eliminated. Following in the same way, we can also conduct an analysis on the BGK model with the D2Q4 lattice, and derive the *numerical* slip $\phi_{s,\mathrm{BGK}}$,

$$\phi_{s,\mathrm{BGK}} = \frac{1 - s_D}{s_D^2}\frac{\Delta\phi}{N^2}. \tag{25}$$

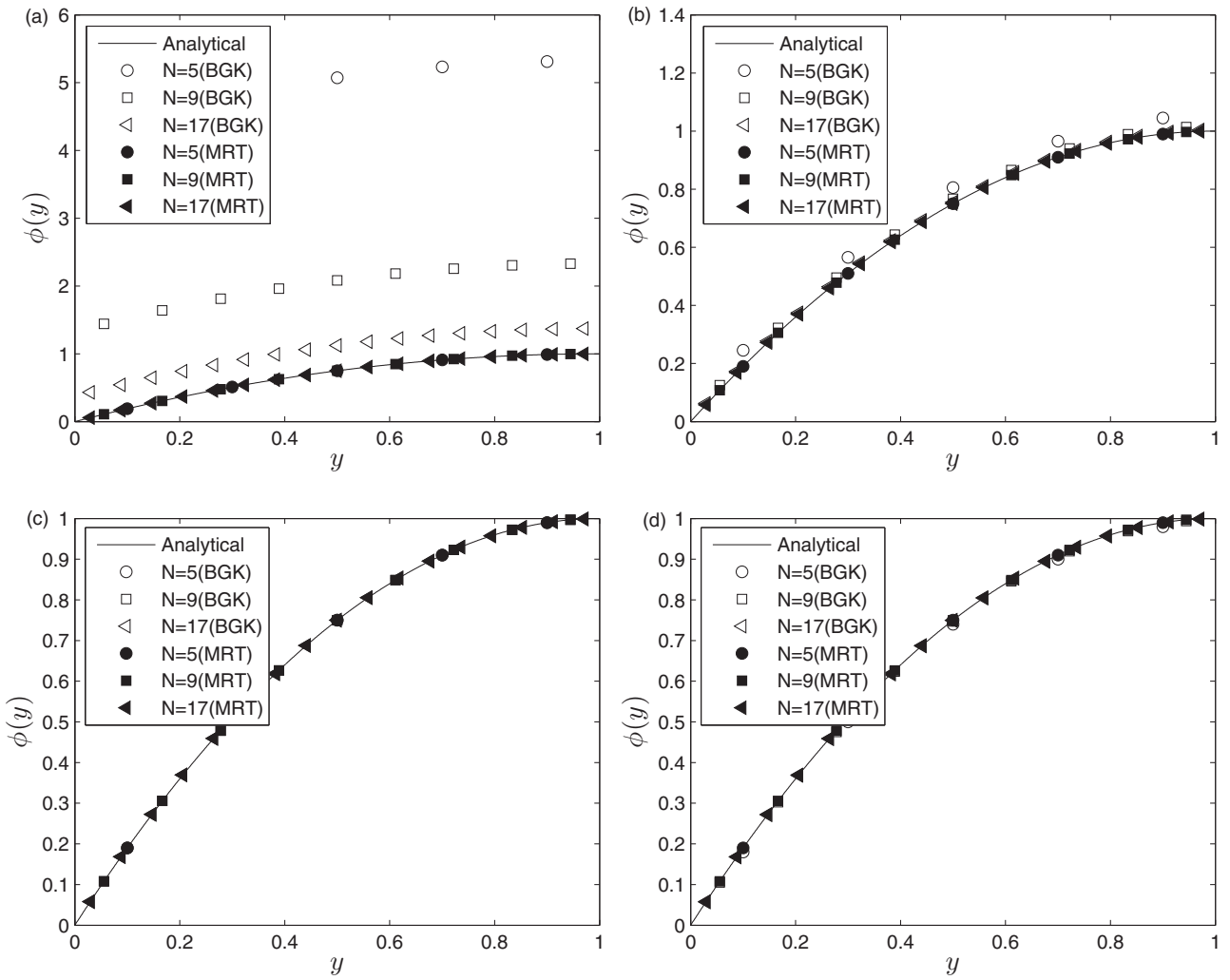

FIG. 4. Numerical results of the BGK and MRT models (D2Q5 lattice) under different lattice sizes and relaxation parameters (a) $s_D = 0.1$, (b) $s_D = 0.6$, (c) $s_D = 2(6 - \sqrt{30})$, and (d) $s_D = 1.9$.

Based on Eq. (25), one can find that the in the BGK model, the HBB boundary condition also has a second-order convergence rate, while usually the numerical slip $\phi_{s,\mathrm{BGK}}$ cannot be eliminated unless $s_D = 1$ which may be not satisfied for a given diffusion coefficient.

Similarly, we also carried out some analysis on the MRT and BGK models with D2Q5 and D2Q9 lattices, and derived the *numerical* slip ϕ_s by the following equations: (26a), (26c), (27a), and (27c).

D2Q5 lattice model:

$$\phi_{s,\mathrm{MRT}} = \frac{s_2 s_1 - 12(s_1 + s_2) + 24}{20 s_1 s_2} \frac{\Delta\phi}{N^2}, \tag{26a}$$

$$s_2 = \frac{12(s_D - 2)}{s_D - 12} \Rightarrow \phi_{s,\mathrm{MRT}} = 0, \tag{26b}$$

$$\phi_{s,\mathrm{BGK}} = \left[\frac{6}{5}\left(\frac{1}{s_D} - \frac{1}{2}\right)^2 - \frac{1}{4}\right]\frac{\Delta\phi}{N^2}, \tag{26c}$$

$$s_D = 2(6 - \sqrt{30}) \Rightarrow \phi_{s,\mathrm{BGK}} = 0. \tag{26d}$$

D2Q9 lattice model:

$$\phi_{s,\mathrm{MRT}} = \frac{s_2 s_1 - 8(s_1 + s_2) + 16}{12 s_1 s_2} \frac{\Delta\phi}{N^2}, \tag{27a}$$

$$s_2 = \frac{8(s_D - 2)}{s_D - 8} \Rightarrow \phi_{s,\mathrm{MRT}} = 0, \tag{27b}$$

$$\phi_{s,\mathrm{BGK}} = \frac{1}{12}\left[4\left(\frac{2}{s_D} - 1\right)^2 - 3\right]\frac{\Delta\phi}{N^2}, \tag{27c}$$

$$s_D = 4(2 - \sqrt{3}) \Rightarrow \phi_{s,\mathrm{BGK}} = 0. \tag{27d}$$

From Eqs. (26) and (27), one can find that similar to the above results of the D2Q4 lattice model, in the MRT model with the D2Q5 or D2Q9 lattice, the discrete effect of the HBB boundary condition ($\phi_{s,\mathrm{MRT}}$) can also be eliminated through tuning the free relaxation parameter s_2, while in the BGK model, it cannot be overcome unless the relaxation parameter s_D is equal to a special value which is different for different lattice model. In addition, we would also like to point out that the results of the MRT model with the D2Q9 lattice [Eqs. (27a)

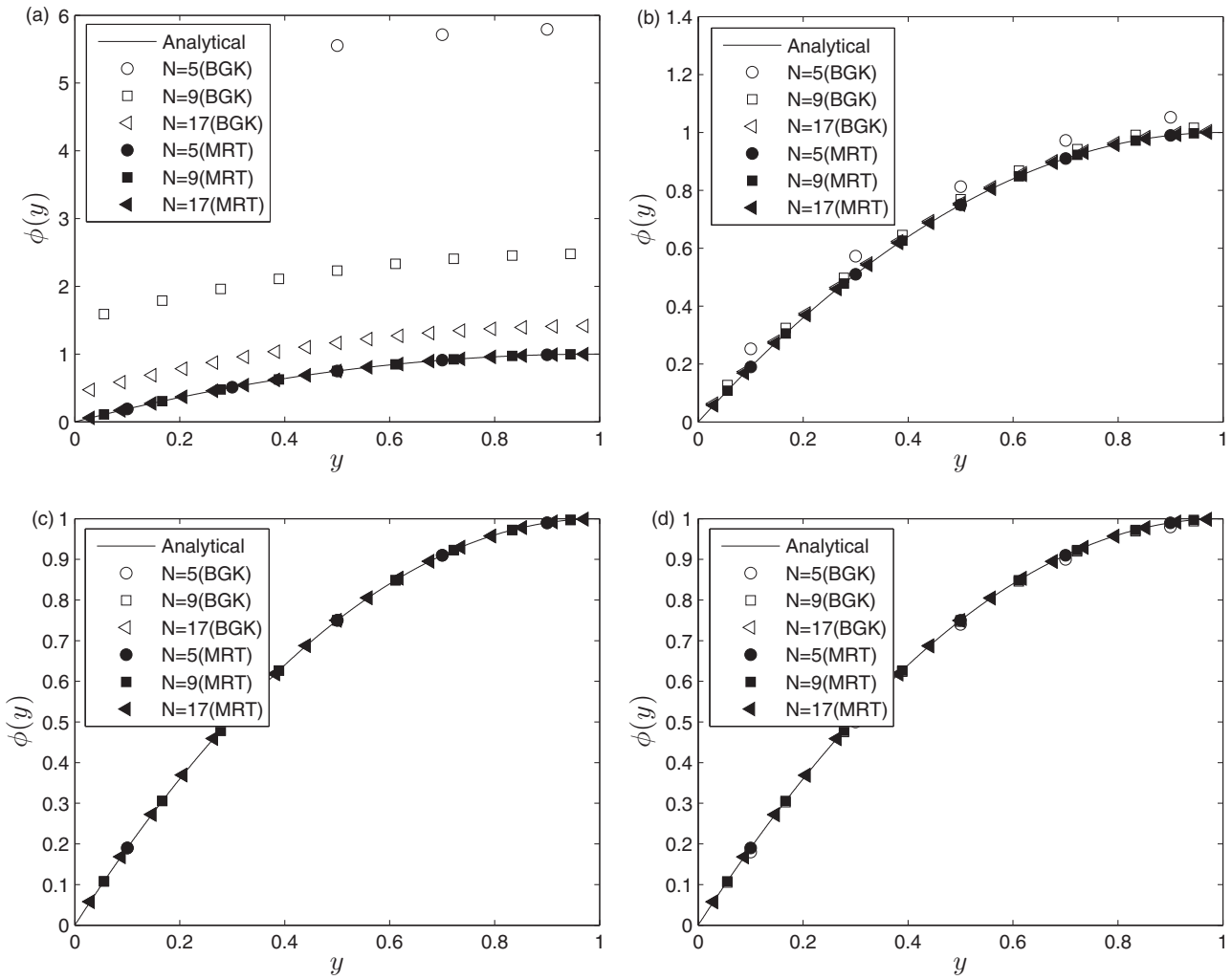

FIG. 5. Numerical results of the BGK and MRT models (D2Q9 lattice) under different lattice sizes and relaxation parameters (a) $s_D = 0.1$, (b) $s_D = 0.6$, (c) $s_D = 4(2 - \sqrt{3})$, and (d) $s_D = 1.9$.

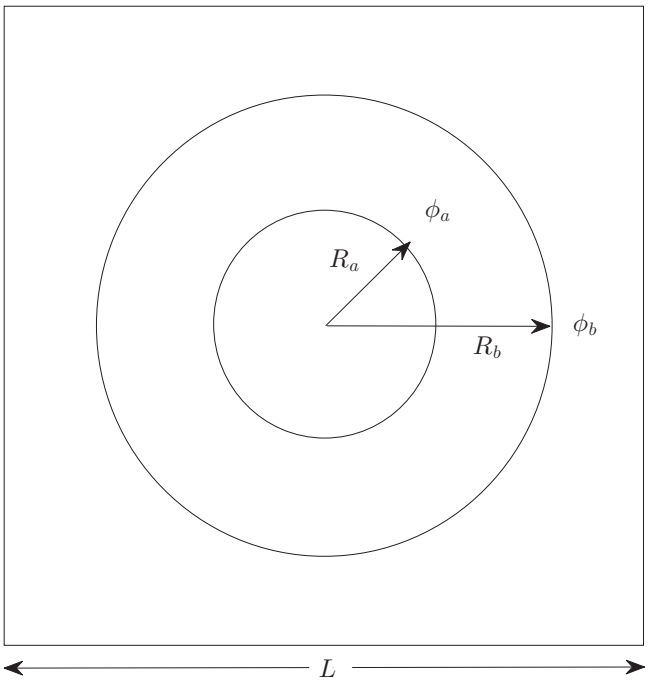

FIG. 6. Schematic of the diffusion between two concentric cylinders.

and (27b)] are similar to those of the MRT model for Poiseuille flow [30,33,35].

IV. NUMERICAL RESULTS AND DISCUSSION

A. Numerical validation

To confirm our above theoretical analysis, we first performed some simulations of the problem shown in Fig. 1 where $L = 1.0$, $u_x = 0.1$, the diffusion coefficient $D = 0.1$, and $\delta x = L/N$ with the grid number N varying from 5 to 17. In our simulations, the periodic boundary condition in the x direction is adopted, and the relaxation parameter s_D is an input variable, and based on Eq. (12), it can be used to determine the time step δt and also the parameter c.

We presented some results with different grid numbers and different values of the relaxation parameter s_D in Figs. 3, 4, and 5. As seen from these figures, it is clear that if the free relaxation parameter s_2 is given by Eq. (24) in the D2Q4 lattice model, Eq. (26b) in the D2Q5 lattice model, or Eq. (27b) in the D2Q9 lattice model, the MRT model can give accurate results even with a very small grid number (e.g., $N = 5$), which is consistent with our theoretical analysis. However, the results of the BGK model cannot match the analytical solutions well unless $s_D = 1$ in the D2Q4 lattice model, $s_D = 2(6 - \sqrt{30})$

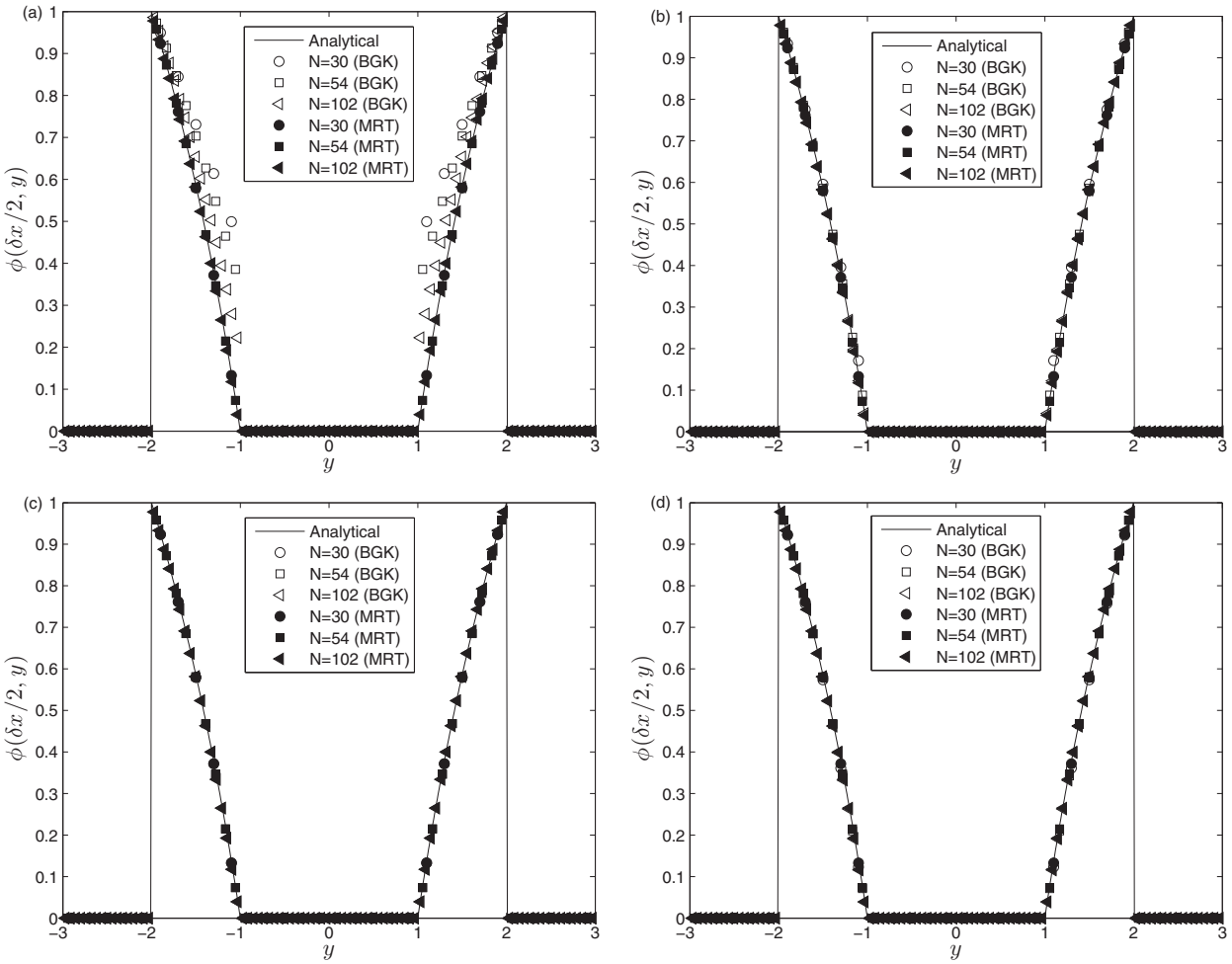

FIG. 7. Numerical results of the BGK and MRT models (D2Q4 lattice) under different lattice sizes and relaxation parameters (a) $s_D = 0.1$, (b) $s_D = 0.6$, (c) $s_D = 1.0$, and (d) $s_D = 1.9$.

in the D2Q5 lattice model, or $s_D = 4(2-\sqrt{3})$ in the D2Q9 lattice model. Actually, for a specified diffusion coefficient, the condition of $s_D = 1$, $s_D = 2(6-\sqrt{30})$, or $s_D = 4(2-\sqrt{3})$ may be not satisfied (for example, if the diffusion coefficient in the CDE is very small, the relaxation parameter s_D in the LB model will approach 2.0), and thus, some discrepancy between the numerical results of the BGK model and the exact solutions are usually observed, especially for a small s_D or a small grid number N. In addition, it is also interesting that $s_D = 2(6-\sqrt{30}) \approx 1.046$ in the D2Q5 model and $s_D = 4(2-\sqrt{3}) \approx 1.072$ in the D2Q9 model are very close to 1.0, which may be the reason why usually $s_D = 1.0$ can give accurate results.

We then tested the above analysis with a more complicated problem, i.e., the steady diffusion between two concentric cylinders. The configuration of the problem can be found in Fig. 6 where two concentric cylinders are located in the center of a square region with the length L. For this problem, Eq. (1) can be written in polar coordinates, and with the help of the following Direchlet boundary conditions,

$$\phi(R_a) = \phi_a, \phi(R_b) = \phi_b, \tag{28}$$

one can obtain the analytical solution to this problem [57],

$$\phi(r) = \frac{\phi_a \ln(R_b/r) + \phi_b \ln(r/R_a)}{\ln(R_b/R_a)}, \quad R_a \leqslant r \leqslant R_b, \tag{29}$$

where R_a and R_b are radii of two cylinders, and ϕ_a and ϕ_b are two constants. In our simulations, the computational region is $[-3,3] \times [-3,3]$ with $L = 6.0$, $R_a = 1.0$, $R_b = 2.0$, $\phi_a = 0.0$, $\phi_b = 1.0$, and the diffusion coefficient D is set to be 0.001. We conducted several simulations with different values of the grid number N, and presented the results in Figs. 7, 8, and 9 in which the D2Q4, D2Q5, and D2Q9 lattice models are adopted. As seen from these figures, if the free relaxation parameter s_2 given by Eq. (24) in the D2Q4 lattice model, Eq. (26b) in the D2Q5 lattice model, or Eq. (27b) in the D2Q9 lattice model is adopted, the results of the MRT model are more accurate than the BGK model, especially for a small s_D or a small grid number N, which is also consistent with our analysis.

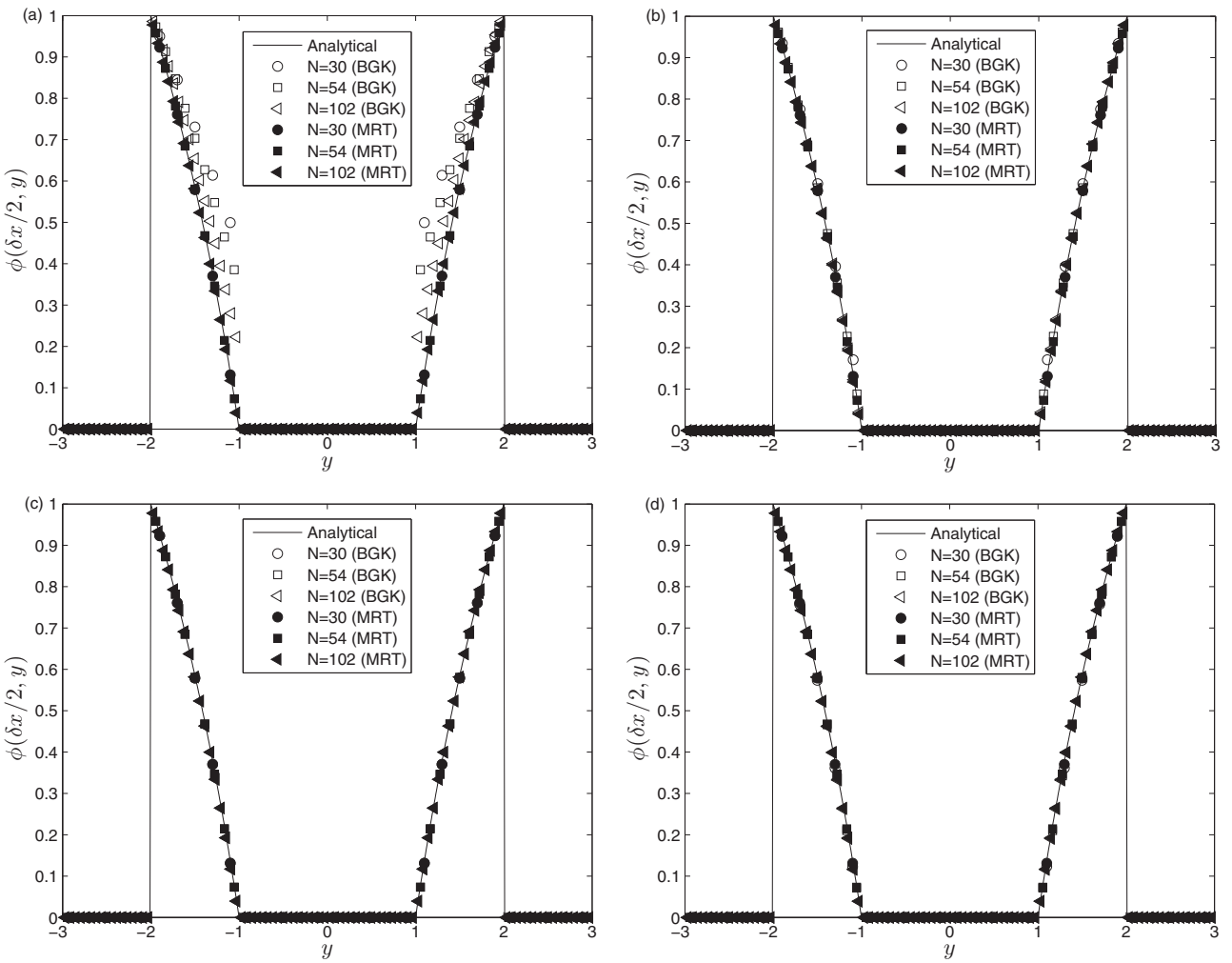

FIG. 8. Numerical results of the BGK and MRT models (D2Q5 lattice) under different lattice sizes and relaxation parameters (a) $s_D = 0.1$, (b) $s_D = 0.6$, (c) $s_D = 2(6-\sqrt{30})$, and (d) $s_D = 1.9$.

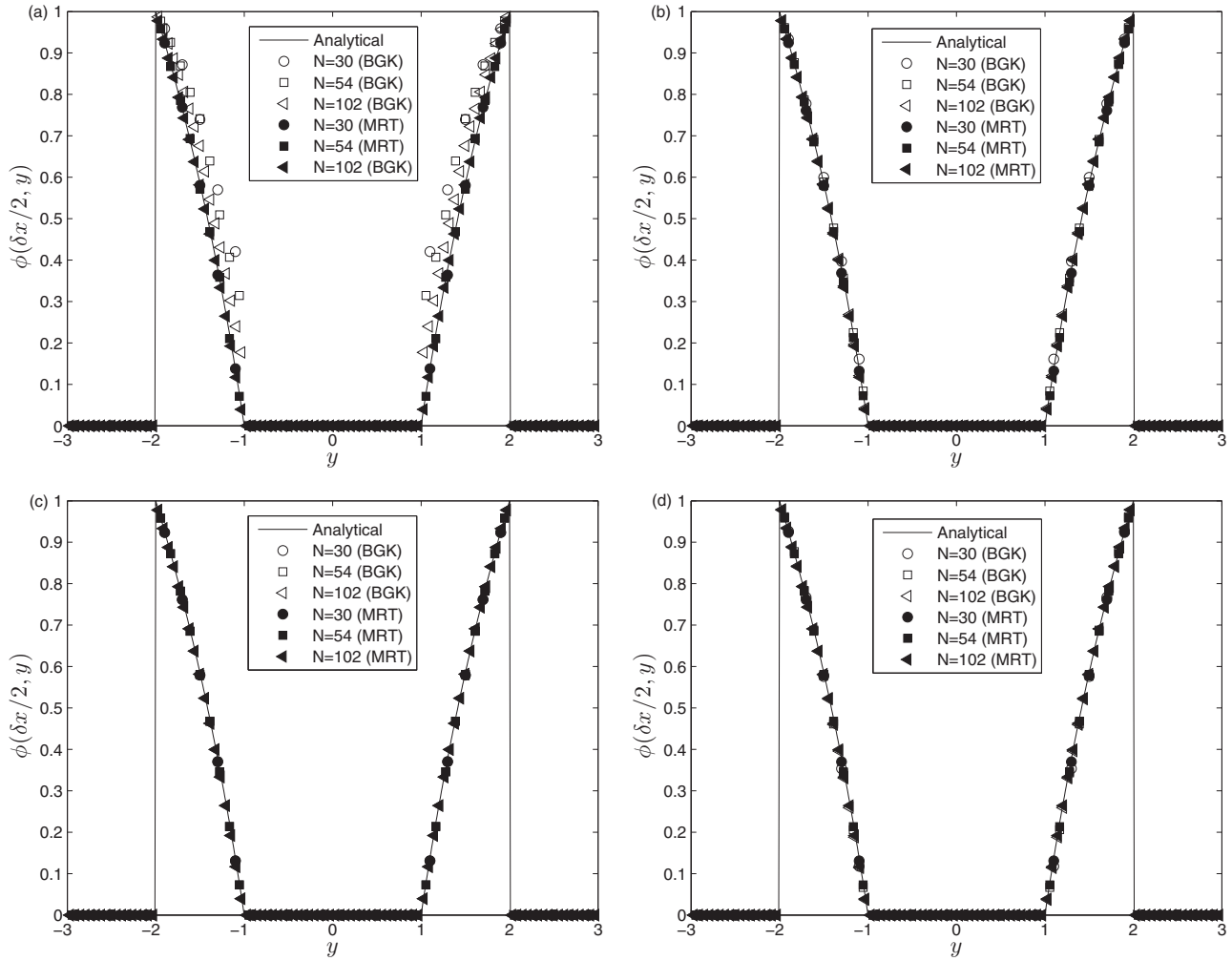

FIG. 9. Numerical results of the BGK and MRT models (D2Q9 lattice) under different lattice sizes and relaxation parameters (a) $s_D = 0.1$, (b) $s_D = 0.6$, (c) $s_D = 4(2-\sqrt{3})$, and (d) $s_D = 1.9$.

B. The relaxation parameter s_2 effect on intrinsic accuracy of the MRT model

We note that the *numerical* slip is caused by the discrete effect of the HBB boundary condition. Therefore, for a periodic problem where the discrete effect of the HBB boundary condition can be excluded, the choice of relaxation time s_2 should have no apparent influence on the numerical results. To confirm this statement, the problem of the Gaussian hill would be studied by the MRT model with the D2Q4 lattice. The problem can be described by Eq. (1) without source term R, and with the proper initial and boundary conditions, one can obtain its analytical solution,

$$\phi(x,y,t) = \frac{\phi_0}{2\pi\left(\sigma_0^2 + 2Dt\right)} \times \exp\left[-\frac{(x-u_x t)^2 + (y-u_y t)^2}{2\left(\sigma_0^2 + 2Dt\right)}\right], \quad (30)$$

where the components of velocity u_x and u_y are two constants. Similar to some available works [15,17,21,23], we also investigated the Gaussian hill problem in a bounded domain $[-1,1] \times [-1,1]$ and adopted the periodic boundary condition on all boundaries. In our simulations, $\sigma_0 = 0.01$ which is small enough to ensure that the periodic boundary condition used is reasonable and accurate at a finite time $T = 10.0$, $\phi_0 = 2\pi\sigma_0^2$,

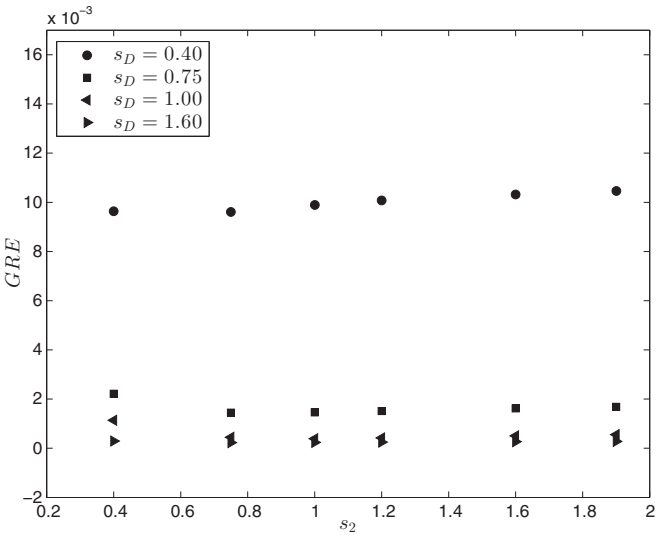

FIG. 10. The effect of relaxation parameter s_2 on the global relative errors.

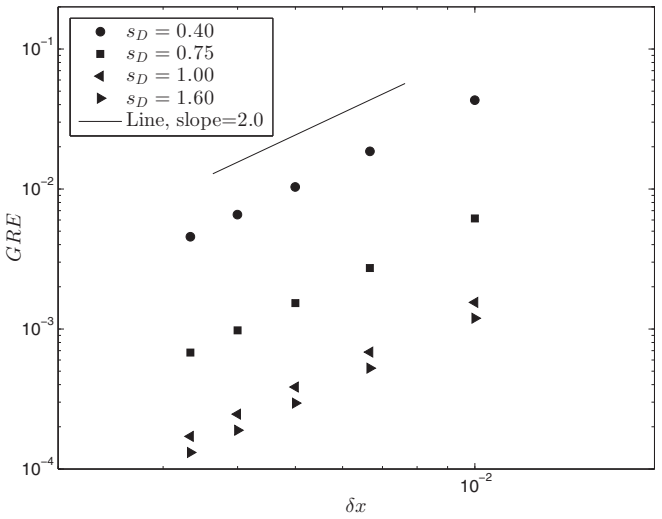

FIG. 11. The global relative errors at different lattice sizes ($\delta x = 1/300, 1/250, 1/200, 1/150$, and $1/100$); the slope of the inserted line is 2.0, which indicates the MRT model has a second-order convergence rate in space.

$D = 0.001$, and $u_x = u_y = 0.01$. To measure the deviation between the numerical results and analytical solutions, the following global relative error (GRE) defined by Eq. (31) is used,

$$\mathrm{GRE} = \frac{\sum_{(x,\,y)} |\phi_a(x,y,t) - \phi_n(x,y,t)|}{\sum_{(x,\,y)} |\phi_a(x,y,t)|}, \tag{31}$$

where the subscripts a and n denote the analytical and numerical solutions. We first tested the effect of relaxation parameter s_2 under different values of s_D, and the results are shown in Fig. 10 where the lattice size is 401×401. As seen from this figure, the relaxation parameter s_2 has some influence on the global relative errors, but its effect is not significant. Based on this result, i.e., the relaxation parameter s_2 has no apparent effect on the numerical results under a specified s_D; we then investigate the influence of relaxation parameter s_2 on the convergence rate of the MRT model with the relation (24). To this end, we performed some simulations under different lattice sizes and different values of s_D, and presented the results in Fig. 11 where the lattice spacing is varied from $1/300$ to $1/100$. From this figure, one can find that the MRT model has a second-order convergence rate in space, and the relaxation parameter s_2 determined by Eq. (24) does not influence the convergence rate of the MRT model. We would also like to point out that in the D2Q5 and D2Q9 lattice models, some similar results are also obtained.

V. CONCLUSIONS

In this work, the discrete effect on the HBB boundary condition of the MRT model for the CDE is analyzed theoretically and numerically. The results clearly show that compared to the BGK model, the free relaxation parameters can be used to improve the accuracy of the MRT model. Particularly, it is also found that the relaxation parameter s_0 corresponding to the conserved variable has no influence on accuracy of the MRT model, and can be chosen arbitrarily, while the effect of the relaxation parameter s_2 corresponding to the second-order moment is very significant. Actually, if the relaxation parameter s_2 is determined by Eq. (24) in the D2Q4 lattice model, Eq. (26b) in the D2Q5 lattice model, or Eq. (27b) in the D2Q9 lattice model, the discrete effect on the HBB boundary condition of the MRT model can be eliminated for the simple problems with a parabolic distribution in one direction, and more accurate results can also be obtained, while in the BGK model, the discrete effect of the boundary condition cannot be removed unless the relaxation parameter s_D is equal to a special value, which may be not satisfied for a given diffusion coefficient. We would also like to point out that although the present analysis is only limited to the HBB boundary condition, it can be extended to other boundary conditions (e.g., the nonequilibrium BB boundary condition [58–60]) of the LB method without any substantial difficulties. Considering the advantages in terms of accuracy and stability, the MRT model would be a better choice in the study of heat and mass transfer during the convection and diffusion process.

ACKNOWLEDGMENTS

The authors would like to thank anonymous referees for their valuable comments and suggestions that improved the quality of this work, and they are also indebted to Prof. Zhaoli Guo for his useful discussions. This work was financially supported by the National Natural Science Foundation of China (Grants No. 51576079 and No. 11272132) and the Natural Science Foundation of Hubei Province (Grant No. 2015CFB440).

APPENDIX A: EQUIVALENT FINITE-DIFFERENCE SCHEME OF THE MRT MODEL

In this Appendix, we will show how to derive the equivalent finite-difference scheme of the MRT model with the D2Q4 lattice. To this end, one can substitute Eq. (6) into Eq. (2) to derive the following equations,

$$f_1^k = f_1^k - \frac{s_0 + 2s_1 + s_2}{4}\left(f_1^k - f_1^{(\mathrm{eq}),k}\right) - \frac{s_0 - s_2}{4}\left(f_2^k - f_2^{(\mathrm{eq}),k}\right) - \frac{s_0 - 2s_1 + s_2}{4}\left(f_3^k - f_3^{(\mathrm{eq}),k}\right) - \frac{s_0 - s_2}{4}\left(f_4^k - f_4^{(\mathrm{eq}),k}\right)$$
$$+ \left(1 - \frac{s_0 + 2s_1 + s_2}{8}\right)\delta t R_1 + \frac{s_2 - s_0}{8}\delta t R_2 + \frac{2s_1 - s_0 - s_2}{8}\delta t R_3 + \frac{s_2 - s_0}{8}\delta t R_4, \tag{A1a}$$

$$f_2^k = f_2^{k-1} - \frac{s_0 - s_2}{4}\left(f_1^{k-1} - f_1^{(\mathrm{eq}),k-1}\right) - \frac{s_0 + 2s_1 + s_2}{4}\left(f_2^{k-1} - f_2^{(\mathrm{eq}),k-1}\right)$$

$$-\frac{s_0-s_2}{4}\left(f_3^{k-1}-f_3^{(\mathrm{eq}),k-1}\right)-\frac{s_0-2s_1+s_2}{4}\left(f_4^{k}-f_4^{(\mathrm{eq}),k-1}\right)$$
$$+\frac{s_2-s_0}{8}\delta t R_1+\left(1-\frac{s_0+2s_1+s_2}{8}\right)\delta t R_2+\frac{s_2-s_0}{8}\delta t R_3+\frac{2s_1-s_0-s_2}{8}\delta t R_4, \tag{A1b}$$

$$f_3^k=f_3^k-\frac{s_0-2s_1+s_2}{4}\left(f_1^k-f_1^{(\mathrm{eq}),k}\right)-\frac{s_0-s_2}{4}\left(f_2^k-f_2^{(\mathrm{eq}),k}\right)-\frac{s_0+2s_1+s_2}{4}\left(f_3^k-f_3^{(\mathrm{eq}),k}\right)-\frac{s_0-s_2}{4}\left(f_4^k-f_4^{(\mathrm{eq}),k}\right)$$
$$+\frac{2s_1-s_0-s_2}{8}\delta t R_1+\frac{s_2-s_0}{8}\delta t R_2+\left(1-\frac{s_0+2s_1+s_2}{8}\right)\delta t R_3+\frac{s_2-s_0}{8}\delta t R_4, \tag{A1c}$$

$$f_4^k=f_4^{k+1}-\frac{s_0-s_2}{4}\left(f_1^{k+1}-f_1^{(\mathrm{eq}),k+1}\right)-\frac{s_0-2s_1+s_2}{4}\left(f_2^{k+1}-f_2^{(\mathrm{eq}),k+1}\right)-\frac{s_0-s_2}{4}\left(f_3^{k+1}-f_3^{(\mathrm{eq}),k+1}\right)$$
$$-\frac{s_0+2s_1+s_2}{4}\left(f_4^{k+1}-f_4^{(\mathrm{eq}),k+1}\right)+\frac{s_2-s_0}{8}\delta t R_1+\frac{2s_1-s_0-s_2}{8}\delta t R_2+\frac{s_2-s_0}{8}\delta t R_3+\left(1-\frac{s_0+2s_1+s_2}{8}\right)\delta t R_4, \tag{A1d}$$

where f_i^k and $f_i^{(\mathrm{eq}),k}$ are the distribution function and its equilibrium part at $y=k\delta x$. It should be noted that Eq. (A1) is only valid for the nodes in the interior of the computational domain ($2\leqslant k\leqslant N-1$), and the nodes $k=1$ and $k=N$ correspond to the first layers near the bottom and top boundaries. Through a summation of Eqs. (A1a) and (A1c), we can obtain

$$f_1^k+f_3^k=\frac{1}{2}\phi_k+\frac{2-s_2}{4s_2}\delta t R, \tag{A2}$$

where Eqs. (3), (4), and (11) have been used. Based on Eqs. (A2) and (11), we can also derive the following equations,

$$f_2^k+f_4^k=\frac{1}{2}\phi_k-\frac{2+s_2}{4s_2}\delta t R, \tag{A3a}$$
$$f_2^{k-1}=\frac{1}{2}\phi_{k-1}-f_4^{k-1}-\frac{2+s_2}{4s_2}\delta t R, \tag{A3b}$$
$$f_4^{k+1}=\frac{1}{2}\phi_{k+1}-f_2^{k+1}-\frac{2+s_2}{4s_2}\delta t R. \tag{A3c}$$

Substituting Eqs. (A2), (A3b), and (A3c) into Eqs. (A1b) and (A1d), we have

$$f_2^k=\left(\frac{1}{2}-\frac{s_1}{4}+s_1\frac{u_{y,k-1}}{2c}\right)\phi_{k-1}+(s_1-1)f_4^{k-1}$$
$$+\frac{s_1s_2+2s_1+2s_2-4}{8s_2}\delta t R, \tag{A4a}$$
$$f_4^k=\left(\frac{1}{2}-\frac{s_1}{4}-s_1\frac{u_{y,k+1}}{2c}\right)\phi_{k+1}+(s_1-1)f_2^{k+1}$$
$$+\frac{s_1s_2+2s_1+2s_2-4}{8s_2}\delta t R. \tag{A4b}$$

After a summation of above two equations, one can derive

$$f_2^k+f_4^k=\left(\frac{1}{2}-\frac{s_1}{4}\right)(\phi_{k-1}+\phi_{k+1})$$
$$+\frac{s_1}{2c}(\phi_{k-1}u_{y,k-1}-\phi_{k+1}u_{y,k+1})$$
$$+(s_1-1)\left(f_2^{k+1}+f_4^{k-1}\right)$$
$$+\frac{s_1s_2+2s_1+2s_2-4}{4s_2}\delta t R. \tag{A5}$$

Based on Eq. (A4), we can rewrite f_2^{k+1} and f_4^{k-1} as

$$f_2^{k+1}=\left(\frac{1}{2}-\frac{s_1}{4}+s_1\frac{u_{y,k}}{2c}\right)\phi_k+(s_1-1)f_4^k$$
$$+\frac{s_1s_2+2s_1+2s_2-4}{8s_2}\delta t R, \tag{A6a}$$
$$f_4^{k-1}=\left(\frac{1}{2}-\frac{s_1}{4}-s_1\frac{u_{y,k}}{2c}\right)\phi_k+(s_1-1)f_2^k$$
$$+\frac{s_1s_2+2s_1+2s_2-4}{8s_2}\delta t R; \tag{A6b}$$

then the following equation can be derived through summing the above two equations,

$$f_2^{k+1}+f_4^{k-1}=\left(1-\frac{s_1}{2}\right)\phi_k+(s_1-1)\left(f_2^k+f_4^k\right)$$
$$+\frac{s_1s_2+2s_1+2s_2-4}{4s_2}\delta t R. \tag{A7}$$

Substituting Eq. (A7) into Eq. (A5) and with the help of Eq. (A3a), one can obtain

$$f_2^k+f_4^k=\left(\frac{1}{2}-\frac{s_1}{4}\right)(\phi_{k-1}+\phi_{k+1})+\frac{s_1-1}{2}\phi_k$$
$$+\frac{s_1}{2c}(\phi_{k-1}u_{y,k-1}-\phi_{k+1}u_{y,k+1})$$
$$+\frac{4s_1s_2-s_2-2}{4s_2}\delta t R. \tag{A8}$$

From the above equation and Eq. (A3a), we can derive the equivalent difference equation (15) of the MRT model.

APPENDIX B: DISCRETE EFFECT OF THE HALFWAY BOUNCE-BACK BOUNDARY CONDITION

In the D2Q4 lattice model, if we substitute the postcollision function f_4^+ at the layer $k = 1$ into the Eq. (22a), one can obtain

$$f_2^1 = \frac{1}{2}\phi_0 - \frac{s_2}{8}\phi_1 + \frac{s_2 - 2s_1}{4} f_2^1 - \left(1 - \frac{2s_1 + s_2}{4}\right) f_4^1 - \frac{6 - s_2}{16}\delta t R, \tag{B1}$$

and also

$$f_2^1 + f_4^1 = \frac{1}{2}\phi_0 - \frac{s_2}{8}\phi_1 + \frac{s_2 - 2s_1}{4}\left(f_2^1 + f_4^1\right) + s_1 f_4^1 - \frac{6 - s_2}{16}\delta t R. \tag{B2}$$

With the help of Eq. (A3a), one can rewrite the above equation as

$$\frac{1}{2}\phi_1 = \frac{1}{2}\phi_0 - \frac{s_1}{4}\phi_1 + s_2 f_4^1 + \frac{s_1 s_2 + 2s_1 - 2s_2 + 4}{8s_2}\delta t R. \tag{B3}$$

Substituting Eq. (A4a) into Eq. (A4b), we can obtain the following equation,

$$f_4^1 = \frac{2 - s_1}{4}\phi_2 + \frac{(2 - s_1)(s_1 - 1)}{4}\phi_1 + (s_1 - 1)^2 f_4^1 + s_1 \frac{s_1 s_2 + 2s_1 + 2s_2 - 4}{8s_2}\delta t R; \tag{B4}$$

then from the above equation, one can also derive f_4^1,

$$s_1 f_4^1 = \frac{1}{4}\phi_2 + \frac{s_1 - 1}{4}\phi_1 + s_1 \frac{s_1 s_2 + 2s_1 + 2s_2 - 4}{8s_2(2 - s_1)}\delta t R. \tag{B5}$$

After the substitution of Eq. (B5) into Eq. (B3), we can derive the relation among ϕ_0, ϕ_1, and ϕ_2,

$$\frac{3}{4}\phi_1 - \frac{1}{4}\phi_2 - \frac{1}{2}\phi_0 = \frac{3s_1 s_2 - 2s_1 - 2s_2 + 4}{4s_2(2 - s_1)}\delta t R. \tag{B6}$$

On the other hand, one can also obtain ϕ_1 and ϕ_2 from the analytical solution of the LB model [Eq. (20)],

$$\phi_1 = \phi_0 + \frac{0.5}{N}\left(2 - \frac{0.5}{N}\right)\Delta\phi + \phi_s, \tag{B7a}$$

$$\phi_2 = \phi_0 + \frac{1.5}{N}\left(2 - \frac{1.5}{N}\right)\Delta\phi + \phi_s. \tag{B7b}$$

Substituting the above two equations into Eq. (B6), we can obtain the *numerical* slip ϕ_s given by Eq. (23).

[1] S. Chen and G. Doolen, Annu. Rev. Fluid Mech. **30**, 329 (1998).
[2] J. Zhang, Microfliud. Nanofluid. **10**, 1 (2011).
[3] Z. Guo and C. Shu, *Lattice Boltzmann Method and Its Applications in Engineering* (World Scientific Publishing Co. Pte. Ltd., Singapore, 2013).
[4] D. Wolf-Gladrow, J. Statist. Phys. **79**, 1023 (1995).
[5] S. P. Dawson, S. Chen, and G. D. Doolen, J. Chem. Phys. **98**, 1514 (1993).
[6] Z. L. Guo, B. C. Shi, and N. C. Wang, J. Sci. Comput. **14**, 291 (1999).
[7] R. G. M. van der Sman and M. H. Ernst, J. Comput. Phys. **160**, 766 (2000).
[8] B. Deng, B. C. Shi, and G. C. Wang, Chin. Phys. Lett. **22**, 267 (2005).
[9] B. C. Shi, B. Deng, R. Du, and X. W. Chen, Comput. Math. Appl. **55**, 1568 (2008).
[10] B. Chopard, J. L. Falcone, and J. Latt, Eur. Phys. J. Spec. Top. **171**, 245 (2009).
[11] H.-B. Huang, X.-Y. Lu, and M. C. Sukop, J. Phys. A **44**, 055001 (2011).
[12] Z. Chai and T. S. Zhao, Phys. Rev. E **87**, 063309 (2013).
[13] J. Perko and R. A. Patel, Phys. Rev. E **89**, 053309 (2014).
[14] H. Yoshida and M. Nagaoka, J. Comput. Phys. **257**, 884 (2014).
[15] Z. Chai and T. S. Zhao, Phys. Rev. E **90**, 013305 (2014).
[16] Q. Li, Z. Chai, and B. Shi, J. Sci. Comput. **61**, 308 (2014).
[17] R. Huang and H. Wu, J. Comput. Phys. **274**, 50 (2014).
[18] X. Zhang, A. G. Bengough, J. W. Crawford, and I. M. Young, Adv. Water Resour. **25**, 1 (2002).
[19] I. Ginzburg, Adv. Water Resour. **28**, 1171 (2005).
[20] I. Rasin, S. Succi, and W. Miller, J. Comput. Phys. **206**, 453 (2005).
[21] H. Yoshida and M. Nagaoka, J. Comput. Phys. **229**, 7774 (2010).
[22] L. Li, R. Mei, and J. F. Klausner, Int. J. Heat Mass Transfer **67**, 338 (2013).
[23] Z. Chai, B. Shi, and Z. Guo, J. Sci. Comput. (2016).
[24] B. Shi and Z. Guo, Phys. Rev. E **79**, 016701 (2009).
[25] S. Suga, Int. J. Mod. Phys. C **17**, 1563 (2006).
[26] C. Huber, B. Chopard, and M. Manga, J. Comput. Phys. **229**, 7956 (2010).
[27] B. Servan-Camas and F. T.-C. Tsai, J. Comput. Phys. **228**, 236 (2009).
[28] B. Servan-Camas and F. T.-C. Tsai, Adv. Water Resour. **31**, 1113 (2008).
[29] I. Ginzburg, Commun. Comput. Phys. **11**, 1439 (2012).
[30] I. Ginzburg and P. M. Adler, J. Phys. II France **4**, 191 (1994).
[31] X. He, Q. Zou, L.-S. Luo, and M. Dembo, J. Stat. Phys. **87**, 115 (1997).
[32] Z. Guo, B. Shi, T. S. Zhao, and C. Zheng, Phys. Rev. E **76**, 056704 (2007).
[33] Z. Guo and C. Zheng, Int. J. Comput. Fluid Dyn. **22**, 465 (2008).
[34] Z. Chai, Z. Guo, L. Zheng, and B. Shi, J. Appl. Phys. **104**, 014902 (2008).
[35] Z. Chai, B. Shi, Z. Guo, and J. Lu, Commun. Comput. Phys. **8**, 1052 (2010).
[36] N. I. Prasianakis, T. Rosén, J. Kang, J. Eller, J. Mantzaras, and F. N. Büchi, Commun. Comput. Phys. **13**, 851 (2013).
[37] S. Ansumali and I. V. Karlin, Phys. Rev. E **66**, 026311 (2002).
[38] S. Succi, Phys. Rev. Lett. **89**, 064502 (2002).

[39] T. Zhang, B. Shi, Z. Guo, Z. Chai, and J. Lu, Phys. Rev. E **85**, 016701 (2012).
[40] R. B. Bird, W. E. Stewart, and E. N. Lightfoot, *Transport Phenomena* (John Wiley & Sons, Inc., New York, 2001).
[41] Y. H. Qian, D. d'Humières, and P. Lallemand, Europhys. Lett. **17**, 479 (1992).
[42] I. V. Karlin, A. Ferrante, and H. C. Öttinger, Europhys. Lett. **47**, 182 (1999).
[43] S. Ansumali, I. V. Karlin, and H. C. Öttinger, Europhys. Lett. **63**, 798 (1999).
[44] S. Ansumali and I. V. Karlin, Phys. Rev. E **62**, 7999 (2000).
[45] S. Ansumali, S. Arcidiacono, S. S. Chikatamarla, N. I. Prasianakis, A. N. Gorban, and I. V. Karlin, Eur. Phys. J. B **56**, 135 (2007).
[46] P. Asinari and I. V. Karlin, Phys. Rev. E **81**, 016702 (2010).
[47] M. Geier, A. Greiner, and J. G. Korvink, Phys. Rev. E **73**, 066705 (2006).
[48] Y. Ning, K. N. Premnath, and D. V. Patil, Int. J. Numer. Meth. Fluids (2015).
[49] P. Lallemand and L. S. Luo, Phys. Rev. E **61**, 6546 (2000).
[50] D. d'Humières, in *Rarefied Gas Dynamics: Theory and Simulations*, edited by B. D. Shizgal and D. P. Weave, Progress in Astronautics and Aeronautics, Vol. 159 (AIAA, Washington, DC, 1992), pp. 450–458.
[51] L.-S. Luo, W. Liao, X. Chen, Y. Peng, and W. Zhang, Phys. Rev. E **83**, 056710 (2011).
[52] Z. Chai and T. S. Zhao, Phys. Rev. E **86**, 016705 (2012).
[53] I. Ginzburg, Adv. Water Resour. **28**, 1196 (2005).
[54] J. Wang, D. Wang, P. Lallemand, and L.-S. Luo, Comput. Math. Appl. **65**, 262 (2013).
[55] Q. Chen, X. Zhang, and J. Zhang, Phys. Rev. E **88**, 033304 (2013).
[56] J. Huang and W.-A. Yong, J. Comput. Phys. **300**, 70 (2015).
[57] H. S. Carslaw and J. C. Jaeger, *Conduction of Heat in Solids* (Clarendon Press, Oxford, 2013).
[58] X. He, S. Chen, and G. D. Doolen, J. Comput. Phys. **146**, 282 (1998).
[59] Q. Kang, D. Zhang, S. Chen, and X. He, Phys. Rev. E **65**, 036318 (2002).
[60] L. Chen, Q. Kang, B. A. Robinson, Y.-L. He, and W.-Q. Tao, Phys. Rev. E **87**, 043306 (2013).